



**Oxide-Mediated Mechanisms of Gallium Foam Generation
and Stabilization during Shear Mixing in Air**

Journal:	<i>Soft Matter</i>
Manuscript ID	SM-COM-03-2020-000503.R1
Article Type:	Communication
Date Submitted by the Author:	25-Apr-2020
Complete List of Authors:	<p>Kong, Wilson; Arizona State University, School for Engineering of Matter, Transport and Energy Shah, Najam Ul Hassan; Arizona State University, School for Engineering of Matter, Transport and Energy Neuman, Taylor; North Carolina State University, Chemical & Biomolecular Vong, Man; North Carolina State University, Chemical & Biomolecular Engineering Kotagama, Praveen; Arizona State University, School for Engineering of Matter, Transport and Energy Dickey, Michael; North Carolina State University, Chemical & Biomolecular Engineering Wang, Robert; Arizona State University, School for Engineering of Matter, Transport and Energy Rykaczewski, Konrad; Arizona State University, School for Engineering of Matter, Transport and Energy</p>

Oxide-Mediated Mechanisms of Gallium Foam Generation and Stabilization during Shear Mixing in Air

*Wilson Kong^{a,**}, Najam Ul Hassan Shah^{a,**}, Taylor V. Neumann^b, Man Hou Vong^b, Praveen Kotagama^a, Michael D. Dickey^b, Robert Y. Wang^{a,*}, and Konrad Rykaczewski^{a,*}*

a. School for Engineering of Matter, Transport and Energy, Arizona State University, Tempe, AZ, 85287, USA

b. Department of Chemical and Biomolecular Engineering, North Carolina State University, Raleigh, NC, 27695

*Corresponding author emails: rywang@asu.edu, konradr@asu.edu

** These authors contributed equally to this research

Keywords: liquid metal, gallium, gallium oxide, metal foam, soft materials

Foaming of gallium-based liquid metals improves their processability and—seemingly in contrast to processing of other metal foams—can be achieved through shear-mixing in air without addition of solid microparticles. Resolving this discrepancy, systematic processing-structure-property characterization demonstrates that many crumpled oxide particles are generated prior to air bubble accumulation.

Non-toxic, room-temperature liquid metals based on gallium (LMs) have many exciting prospective applications in the realms of soft, stretchable, and wearable technology.¹ However, their potential is unlikely to be realized until their high cost, weight, and manufacturing issues are addressed. These processing issues stem from gallium's intrinsic high density, high surface tension, and rapid oxidation in air. For example, without complex processing tricks, metal extruded from a nozzle forms droplets instead of useful shapes such as wires.² Recent reports show that the addition of particles or air bubbles to LM augments its adhesion and rheology which enables deposition and patterning onto many substrates using tools ranging from paintbrushes and stencils to 3D printer nozzles.³⁻⁸ The creation of LM foams through incorporation of air bubbles is particularly compelling because these materials retain fluid or "paste-like" characteristics and metallic properties while having a substantially lower metal content (*i.e.*, density and cost). In addition, the foam can be formed simply through stirring of the LM in air⁹ (please note that if another liquid would be present, the LM would break-up into micro-droplets¹⁰⁻¹³). From a fundamental perspective, this observation is intriguing as many decades of research has shown that the addition of solid micro-particles prior to mixing is required for foaming of high melting temperature metals.¹⁴ While the bubble-stabilizing micro-particles are typically spheroidal and ceramic (*e.g.* silicon carbide), aluminum foams formed through compacting and melting aluminum powder can also be stabilized by the oxide film present on the powder prior to processing.¹⁵ In this work, we systematically show that the structure-property-processing relationships for shear mixing of liquid gallium in air stem from the generation and incorporation of crumpled gallium-oxide flakes within the LM during processing.

We fabricated the LM foams by melting 100 g of gallium (99.99% from Rotometals) at 35 to 40°C in a 50 mL beaker and mixing it in air at 600 rpm using an industrial mixer⁵ outfitted with a

3D printed cross-shaped impeller (see Fig. S1 in ESI for experimental details). From a qualitative point of view, the images in Fig.1a show that extended mixing of the LM results in physical transformation of the homogeneous liquid (lustrous cross-section) into a highly heterogenous foam (diffusely reflecting cross-section). To gain an insight into the metal foaming process, we used a high-speed camera (a Photron FastCam mini UX-100) mounted at a 45-degree angle to image the surface of the LM during mixing. As during mixing of aqueous foams,¹⁶ shearing in both early (Movie 1) and later (Movie 2) stages of the process generates high-amplitude waves and large ripples on the surface of the LM. Some of these waves fold onto themselves, creating cavities that later become air bubbles within the LM (see Fig.1b and Fig.S2 in ESI). The presence of the air bubbles is evident in the internal structure of the solidified gallium foam (see Fig.1a). A closer inspection of the LM surface during mixing exposes a feature that is absent in aqueous foams: the surface consists of microscopic “islands” surrounded by a lustrous “sea”. The diffuse light reflection from the islands reveals their material composition. Specifically, such reflection is characteristic of the 1-3 nm thin gallium oxide skin¹⁷ that has wrinkled on nano- and micro-scales due to underlying liquid motion.¹⁸ The shear stresses associated with the stirring process fractures the continuous “old” oxide film into floating oxide-islands (see Fig.1c). We have previously induced and imaged analogous behavior in a more-controlled fashion by rastering a focused ion beam over the LM surface (see Fig.1d).¹⁹ Even in high vacuum conditions (10^{-4} Pa), a new, thin oxide begins to form in-between fractured “old” oxide islands within seconds. In atmospheric conditions this process is much quicker, with new oxide emerging in 10^{-5} to 10^{-3} s.²⁰⁻²² However, presumably due to the adsorption, dissociation, and surface diffusion of oxygen molecules,²¹ at least in vacuum the new oxide grows in a non-uniform fractal-like manner. Consequently, much of the surface in-between the “old” oxide micro-islands consist of a very thin and unwrinkled oxide

that is highly light-reflecting (or transparent) in nature. Intriguingly, either through macroscopic surface-to-bulk flow near the impeller or through microscopic buckling of the surface waves, many of these islands are internalized as oxide-flakes into the bulk of the LM.

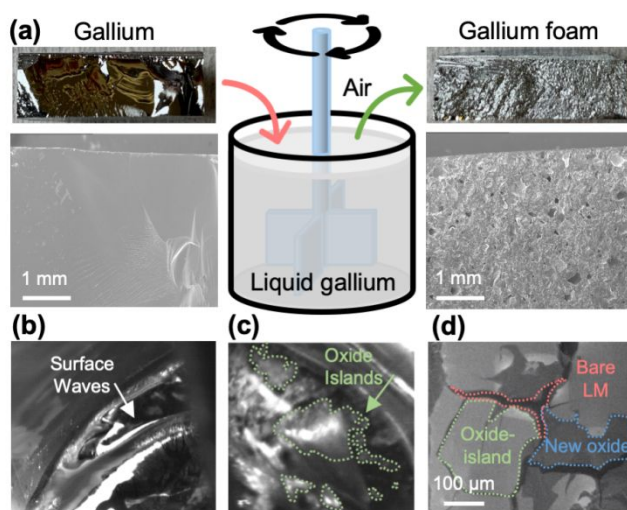
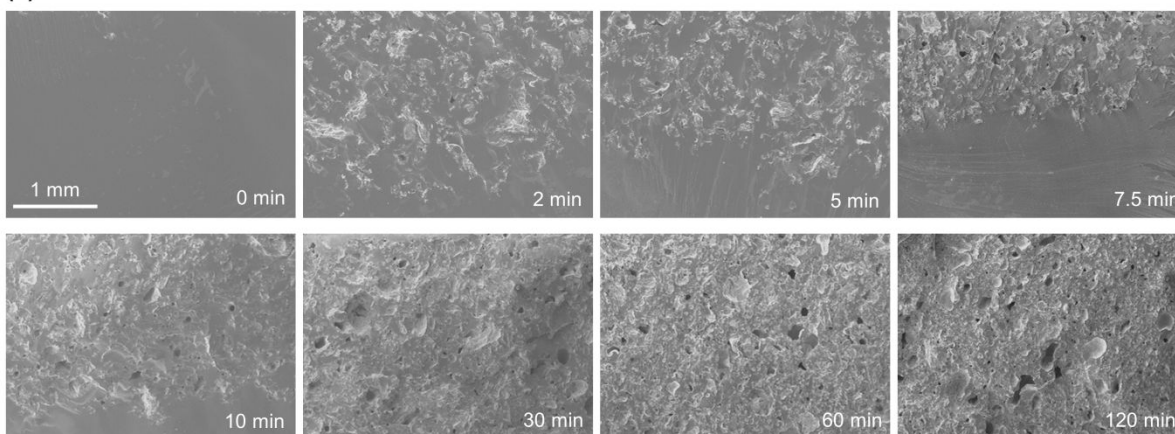


Fig. 1. (a) Schematic of gallium foam fabrication showing light and electron microscopy images of pure gallium and gallium foam made through shear-mixing of liquid gallium in air; (b-c) high-speed camera images showing (b) surface waves and (c) gallium-oxide islands on the surface of the stirred LM; (d) focused ion beam image showing oxide-islands generated through ion ablation on the surface of LM in vacuum.

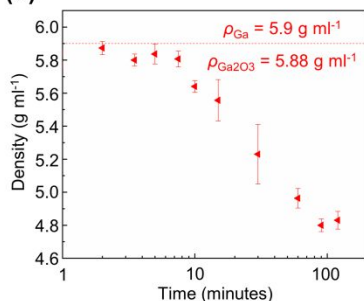
To evaluate the bulk composition of the mixed LM, we used a scanning electron microscope (Amray 1910 FESEM employing 20 kV accelerating voltage) to image cross-sections of LM samples that were stirred for 0, 2, 3.5, 5, 7.5, 10, 15, 30, 60, 90, and 120 minutes prior to freezing (the samples were simply cleaved with a razor blade). After 2 minutes of mixing, the previously smooth internal surface of the unmixed gallium contains a large concentration of oxide flakes (see Fig.2a and Fig.S6 in ESI). Through internal shearing or prior wrinkling on the LM surface, many of these flakes have crumpled and resemble three-dimensional particles^{5,6,8} that can be thought of as microscopic analogs of crumpled paper. The magnified cross-section of one of such particles

obtained using cryogenic focused ion beam cross-sectioning^{23,24} shows that the crumpled oxide flakes have many, often nanoscale, air voids captured within them (see Fig. S5). As a result, the crumpled flakes are slightly buoyant and are mostly suspended near the top of the sample block. Stirring of the LM for another five minutes predominantly leads to accumulation of more of the oxide particles. It is not until 7.5 minutes of mixing that a population of microscopic ($\gg 10 \mu\text{m}$) air bubbles can be observed. Since they are surrounded by a thin oxide layer, we will refer to these bubbles as air capsules. LM mixing times between 10- and 30-minutes results in an increased number of the air capsules, which are buoyant and rise to the surface of the sample block. If mixing is continued for longer time (up to 120 minutes), the air capsules and oxide flakes appear to be present in the entire volume of the LM. Naturally, the accumulation of oxide flakes and air capsules significantly alters physical properties of the foams, and we quantify these properties next.

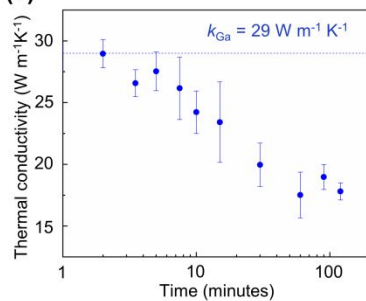
(a)



(b)



(c)



(d)

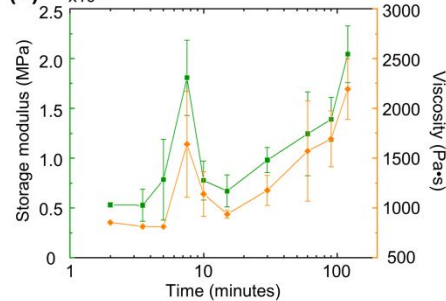


Fig. 2. (a) Cross-sectional SEM images of gallium mixed at different times with the top row times corresponding to the oxide accumulation period and the bottom row showing proper foaming process with bubble stabilization and accumulation (top of the image corresponds to physical top of the sample); (b-d) plots showing the (b) density, (c) thermal conductivity, and (d) storage modulus and viscosity of gallium as a function of the shear-mixing time.

For each of the mixing times, we measured density, thermal conductivity, viscosity as well as loss and storage moduli of the stirred liquid metal. To measure the density of each sample, we employed the Archimedes principle.²⁵ Specifically, we cast circular disks of gallium with a 2 cm diameter and a 6 mm thickness using a polymer mold. We then measured the buoyant force by suspending the disk in a container of water on an analytical balance (see section S2 in ESI for more details). Despite the evident incorporation of many oxide flakes, the density value for the first 7.5 minutes of stirring remains near the 5.9 g ml⁻¹ density of pure gallium (red dotted bar in Fig.2b). This discrepancy can be resolved by pointing out that the density of the predominant gallium oxide skin phase,²⁶ β -Ga₂O₃ is also 5.88 g ml⁻¹.²⁷ Most likely the density value we measured is slightly smaller than that of Ga or β -Ga₂O₃ because of the presence of nanoscale air pockets in the crumpled oxide flakes. If stirring is continued for more than 7.5 minutes, the density of the material begins to decrease substantially, eventually reaching 4.8 g ml⁻¹ after 2 hours of mixing. Based on our structural characterization, this mixing time threshold for density decrease stems from the initiation of air capsule accumulation in the LM.

In contrast to the initially unchanged value of density, the plot in Fig.2c shows that the thermal conductivity of the LM begins to decrease shortly after the onset of the shear-mixing process. We measured this property using a thermal reference bar method following the modified ASTM D5470 standard (see sections S2 and S4 in ESI for more details).^{28,29} Please note that we measured the thermal rather than electrical conductivity because the latter has been previously shown to be only

mildly impacted by LM stirring.⁵ In contrast, thermal conductivity decreases, even after just 2 to 5 minutes stirring, from $29 \text{ Wm}^{-1}\text{K}^{-1}$ (pure gallium) and reaches $18 \text{ Wm}^{-1}\text{K}^{-1}$ after 2 hours of mixing (could decrease to $2 \text{ Wm}^{-1}\text{K}^{-1}$ after 36 hours of mixing³⁰). We note that the exact mixing time at which the thermal conductivity starts changing is difficult to establish because the initial change is comparable to the experimental uncertainty. In light of our structural characterization, these measurements demonstrate that both the oxide flakes and air capsules significantly disrupt thermal energy carrier transport. Owing to the continuous metal matrix, however, the LM foam thermal conductivity is still higher than that of elastomer composites with liquid metal inclusions.^{12,29,31,32}

As with thermal conductivity, the rheological properties of the LM are also significantly impacted through shear mixing. We measured these properties using a rheometer equipped with a 40 mm parallel plate geometry (see section S2 in ESI for more details). Since the dispersal of oxide flakes throughout the bulk LM phase is analogous to loading of solid particle fillers to the system, it yields an immediate increase in both viscosity and storage modulus (G'), as seen in the plot in Fig. 2d. A similar trend is observed with the loss modulus (G''). The loss modulus is not depicted here as the elastic behavior associated with the storage modulus is of more direct interest, however both are plotted together in Fig. S3 in ESI. The loss modulus was consistently 20-30 times smaller than the storage modulus. The storage modulus and viscosity reach an initial peak at 7.5 minutes of stirring (1.5 MPa and 1600 Pa.s, respectively). The peak at 7.5 minutes corresponds with the point just before many air pockets start being incorporated into the foam. Further mixing results in a rapid drop in the viscosity and modulus, presumably in response to the inclusion air as a “soft” filler. With continued mixing, the modulus and viscosity increase, reaching eventual values of 2.04×10^{-3} and 2193 Pa.s, respectively, at a mixing time of 120 minutes. Increased mixing time

results in more oxide flakes and air pockets being encapsulated, which has been shown in prior literature to result in an increase in material modulus and viscosity.³³

In summary, our structural and property characterization of shear-mixed liquid gallium shows that like high-melting point metals,^{14,15} near room-temperature LMs require a small volume fraction of solid particles in order to foam. In the case of the LMs, however, the solid particles are not added prior to stirring but are generated during the process by fracturing and internalizing the thin native oxide film on liquid-air interface. In our setup about 7.5 minutes of mixing is required to accumulate a critical volume fraction of oxide flakes, which crumple into three-dimensional particles that can contain nanoscale air voids, prior to air bubble formation and stabilization. With a different mixing arrangement, this time period might be different. The density, thermal, and rheological properties of gallium foam are highly impacted by the inclusion of oxide flakes and air bubbles. While in general the density and the thermal conductivity decrease, the viscosity and storage modulus first peak and then continue to increase with the stirring time. These alterations to density and rheology are advantageous for processing, dispensing, and application of the foams.

Although a general explanation for the foam stabilizing role of particles has not been agreed on, our structural characterization supports notions of bubble interface stabilization as well as physical bridging of bubbles.¹⁴ Specifically, the representative SEM images in Fig.3 show that besides oxide encapsulating air pockets, some oxide flakes can extend in-between two such voids. It is important to note that the structure of the LM foams is highly dynamic and most of the geometrical feature will change during the mixing and application process. For example, air capsules can coalesce, split or even collapse. This leads to cavities with irregular shapes and a wide range of air capsule sizes. From an application perspective, this random and unpredictable structure is undesirable because it likely restricts the range of possible properties for the foams.

Although not an issue when utilizing pure gallium, the formation of many oxide structures reduces gallium content and in the case of LM alloys could lead to shift from eutectic compositions. Based on the insight from our work, these problems could likely be alleviated by adding a small fraction of particles to LMs prior to shear mixing or even direct bubble injection. Such novel processing methods could improve the LM foam structure and properties yielding a truly multifunctional soft material.

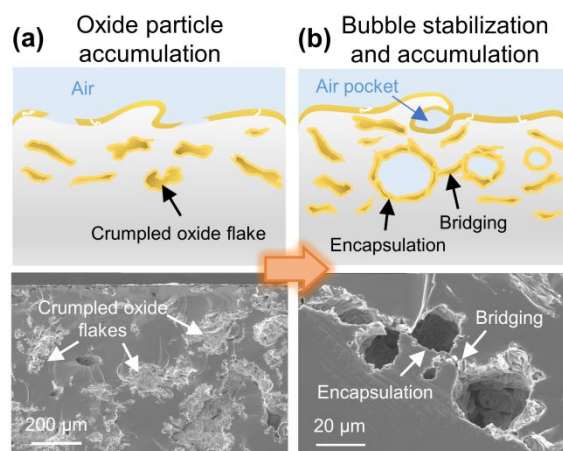


Fig. 3. Schematic of liquid gallium foaming mechanisms: (a) oxide flake accumulation stage where surface oxides fractured during mixing are incorporated into the bulk LM and crumple into pseudo-three-dimensional particles; (b) oxide-mediated entrapment of air during shear mixing with subsequent bubble stabilization and accumulation.

Acknowledgments

KR and RYW acknowledge financial support from the Semiconductor Research Corporation contract #2017-PK-2787 and Arizona State University. NUHS acknowledges support of the Fulbright-HEC Scholarship program. MDD and TN acknowledge support from the National Science Foundation (ERC EEC-1160483).

We gratefully acknowledge the use of the characterization equipment within the LeRoy Eyring Center for Solid State Science at Arizona State University.

References

- 1 M. D. Dickey, *Adv. Mater.*, 2017, **29**, 1606425.
- 2 A. Cook, D. P. Parekh, C. Ladd, G. Kotwal, L. Panich, M. Durstock, M. D. Dickey and C. E. Tabor, *Adv. Eng. Mater.*, 2019, **21**, 1900400.
- 3 W. Kong, Z. Wang, M. Wang, K. C. Manning, A. Uppal, M. D. Green, R. Y. Wang and K. Rykaczewski, *Adv. Mater.*, 2019, **31**, 1904309.
- 4 U. Daalkhaijav, O. D. Yirmibesoglu, S. Walker and Y. Mengüç, *Adv. Mater. Technol.*, 2018, **3**, 1700351.
- 5 X. Wang, L. Fan, J. Zhang, X. Sun, H. Chang, B. Yuan, R. Guo, M. Duan and J. Liu, *Adv. Funct. Mater.*, 2019, 1907063.
- 6 H. Chang, R. Guo, Z. Sun, H. Wang, Y. Hou, Q. Wang, W. Rao and J. Liu, *Adv. Mater. Interfaces*, 2018, **5**, 1800571.
- 7 H. Wang, B. Yuan, S. Liang, R. Guo, W. Rao, X. Wang, H. Chang, Y. Ding, J. Liu and L. Wang, *Mater. Horizons*, 2018, **5**, 222–229.
- 8 B. Yuan, C. Zhao, X. Sun and J. Liu, *Adv. Funct. Mater.*, 2020, 1910709.
- 9 X. Wang, W. Yao, R. Guo, X. Yang, J. Tang, J. Zhang, W. Gao, V. Timchenko and J. Liu, *Adv. Healthc. Mater.*, 2018, 1800318.
- 10 I. D. Tevis, L. B. Newcomb and M. Thuo, *Langmuir*, 2014, **30**, 14308–14313.
- 11 A. Martin, B. S. Chang, Z. Martin, D. Paramanik, C. Frankiewicz, S. Kundu, I. D. Tevis and M. Thuo, *Adv. Funct. Mater.*, 2019, **29**, 1903687.
- 12 R. Tutika, S. H. Zhou, R. E. Napolitano and M. D. Bartlett, *Adv. Funct. Mater.*, 2018, 1804336.
- 13 R. Tutika, S. Kmiec, A. B. M. T. Haque, S. W. Martin and M. D. Bartlett, *ACS Appl. Mater. Interfaces*, 2019, **11**, 17873–17883.
- 14 J. Banhart, *Adv. Eng. Mater.*, 2006, **8**, 781–794.
- 15 C. Körner, M. Arnold and R. F. Singer, *Mater. Sci. Eng. A*, 2005, **396**, 28–40.
- 16 N. Politova, S. Tcholakova, Z. Valkova, K. Golemanov and N. D. Denkov, *Colloids Surfaces A Physicochem. Eng. Asp.*, 2018, **539**, 18–28.
- 17 Z. J. Farrell and C. Tabor, *Langmuir*, 2018, **34**, 234–240.
- 18 S. Liu, X. Sun, N. Kemme, V. G. G. Damle, C. Schott, M. Herrmann and K. Rykaczewski, *Microfluid. Nanofluidics*, 2016, **20**, 1–6.
- 19 K. Doudrick, S. Liu, E. M. E. M. Mutunga, K. L. K. L. Klein, V. Damle, K. K. K. Varanasi and K. Rykaczewski, *Langmuir*, 2014, **30**, 6867–6877.
- 20 A. Plech, U. Klemradt, H. Metzger and J. Peisl, *J. Phys. Condens. Matter*, 1998, **10**, 971.

- 21 J. M. Chabala, *Phys. Rev. B*, 1992, **46**, 11346.
- 22 Y. Chen, J. L. Wagner, P. A. Farias, E. P. DeMauro and D. R. Guildenbecher, *Int. J. Multiph. Flow*, 2018, **106**, 147–163.
- 23 N. Antoniou, K. Rykaczewski and M. D. Uchic, *MRS Bull.*, 2014, **39**, 347–352.
- 24 K. Rykaczewski, S. Anand, S. B. S. B. Subramanyam and K. K. K. Varanasi, *Langmuir*, 2013, **29**, 5230–5238.
- 25 A. B. Spierings, M. Schneider and R. Eggenberger, *Rapid Prototyp. J.*, 2011, **17**, 380–386.
- 26 M. J. Regan, P. S. Pershan, O. M. Magnussen, B. M. Ocko, M. Deutsch and L. E. Berman, *Phys. Rev. B*, 1997, **55**, 15874–15884.
- 27 B. Bayraktaroglu, *Air Force Res. Lab. Sensors Dir. WPAFB United States*, 2017, **No. AFRL-R**, 1–103.
- 28 D. R. Thompson, S. R. Rao and B. A. Cola, *J. Electron. Packag.*, 2013, **135**, 41002.
- 29 M. Ralphs, W. Kong, R. Y. Wang and K. Rykaczewski, *Adv. Mater. Interfaces*, 2019, **6**, 1801857.
- 30 L. Zhao, S. Chu, X. Chen and G. Chu, *Bull. Mater. Sci.*, 2019, **42**, 192.
- 31 M. D. Bartlett, N. Kazem, M. J. Powell-Palm, X. Huang, W. Sun, J. A. Malen and C. Majidi, *Proc. Natl. Acad. Sci.*, 2017, **114**, 2143–2148.
- 32 M. I. Ralphs, N. Kemme, P. B. Vartak, E. Joseph, S. Tipnis, S. Turnage, K. N. Solanki, R. Y. Wang and K. Rykaczewski, *ACS Appl. Mater. Interfaces*, 2018, **10**, 2083–2092.
- 33 M. C. Tan, N. L. Chin, Y. A. Yusof, F. S. Taip and J. Abdullah, *Int. dairy J.*, 2015, **43**, 7–14.

The fracturing and incorporation of liquid gallium surface oxides during shear mixing in air enables the stabilization of air bubbles within gallium which leads to the formation of a room-temperature liquid metal foam.

